Electrochimica Acta 291 (2018) 362–372

Contents lists available at ScienceDirect

Electrochimica Acta

journal homepage: www.elsevier.com/locate/electacta

Polypyrrole doped with dodecylbenzene sulfonate as a protective coating for copper

Ursula Carragher, Carmel B. Breslin*

Department of Chemistry, Maynooth University, Maynooth, Co. Kildare, Ireland

A R T I C L E I N F O

Article history:
Received 6 July 2018
Received in revised form
28 August 2018
Accepted 29 August 2018
Available online 1 October 2018

Keywords:
Corrosion protection
Copper
Dodecylbenzene sulfonate
Polypyrrole
Tartrate

A B S T R A C T

Polypyrrole doped with dodecylbenzene sulfonate (DBS) was formed at copper, PPy–DBS, and at a thin coating of polypyrrole doped with tartrate to form a bilayer of PPy–Tar/PPy–DBS at copper. The two polymer coatings showed good protective properties. Breakdown potentials of 0.85 V and 0.93 V vs SCE were recorded in 0.1 M NaCl for the PPy–DBS and PPy–Tar/PPy–DBS bilayer, respectively. The more protective properties of the bilayer were explained in terms of an adherent thin polymer that was formed in the tartrate solution without significant dissolution of copper before the polymer was nucleated. The protective properties were also evident from open-circuit potential measurements where the potential adopted by the polymer coated copper remained constant and higher than the potential of the uncoated copper for several days. Furthermore, a decrease in the corrosion current density was observed from 1.95 $\mu A\ cm^{-2}$ for copper to 0.12 $\mu A\ cm^{-2}$ for the bilayer. The concentration of DBS had an influence on the properties of the polymer films with more protective films formed in 0.05 M DBS. The critical micelle concentration of DBS in 0.3 M pyrrole was measured as 9.8 mM, indicating a relatively high level of micelles in 0.05 M DBS. The protective properties of the coating were attributed to the large and immobile DBS anion, which gives the polymer cation exchange properties, minimising the uptake of chloride anions. In addition, the incorporation of anionic micelles may occur to repel further the chloride anions.

1. Introduction

It is well known that oxidation and corrosion of copper occurs and this is particularly evident in chloride–containing solutions or environments. It is generally thought that a Cu_2O phase is deposited initially during oxidation, followed by the formation of Cu(II) compounds, such as cupric hydroxide ($Cu(OH)_2$) and cupric oxide (CuO) [1]. A pseudo–passive film is generated due to the formation of a $Cu(OH)_2$ film filling the pores of the base film. Shoesmith et al. [2] have demonstrated that $Cu(OH)_2$ forms in two layers, a base layer grown by a solid–state mechanism and an upper layer of individual crystals nucleated and grown from solution. In the presence of chloride anions, and when conditions favour interactions of chloride ions with the oxide film, this layer becomes less protective, and the breakdown potential is displaced to more negative potentials [3].

Various inhibitors [4,5] have been used to minimise the corrosion of copper, but in more recent times conducting polymers, primarily polypyrrole, have been employed [6–14]. The electropolymerisation of pyrrole, which requires the oxidation of the monomer, to generate polypyrrole occurs at potentials in the vicinity of 0.60 V–0.80 V vs SCE and at these potentials dissolution of copper occurs. These dissolution reactions can be minimised by selecting anions that form complexes with Cu^{2+} inhibiting further dissolution and enabling the formation of the polymer. Polypyrrole has been formed at copper from oxalate, salicylate, phosphate, phytic acid, benzoate and citrate [6–14], while polymers formed using substituted pyrrole monomers, such as methyl pyrrole, have also been formed [15–17] to give protective properties to the copper substrate. Corrosion protective coatings have been obtained with poly(o–toluidine) coatings deposited at copper from oxalate or salicylate [18–20], while the polypyrrole matrix has also been modified with polyhedral oligomeric silsesquioxane [21] and deposited metals [22].

Many of the dopants used such as oxalate, citrate, benzoate, salicylate and phosphate are relatively small and mobile. These are incorporated as dopants during the formation of the polypyrrole

---

* Corresponding author.
E-mail address: Carmel.Breslin@mu.ie (C.B. Breslin).

https://doi.org/10.1016/j.electacta.2018.08.155
0013-4686/© 2018 Elsevier Ltd. All rights reserved.

film, but they are expelled on reduction of the film, facilitating anion exchange with chloride anions. On the other hand, phytic acid, a large cyclic acid, has been shown to inhibit the dissolution of copper by acting as a cation exchange membrane [12,13]. On reduction of the polypyrrole matrix, cations enter the film as the large immobile anion is not expelled. Dodecyl benzene sulfonate (DBS) is another large dopant that shows cation exchange properties when doped within polypyrrole. It has been used to form polypyrrole at inert substrates [23]. Furthermore, it was used by Hien et al. [24] to deposit an inner layer of PPy–DBS at mild steel, while Prissanaroon et al. [25] formed PPy–DBS on electropolished copper at potentials higher than 1.5 V vs SCE to study the interface between copper and the polymer for potential application in electronics and sensing. The corrosion protective properties of the film were not considered. In addition to being large, DBS is well known as a surfactant and it has the ability to form micelles [26,27]. In polar solvents, such as water, the DBS monomers assemble to form a micelle with their hydrocarbon tails located in the core of the micelle and shielded from the polar water, while the polar SO_3^- groups project outwards into the bulk solution.

The DBS was selected in this study because it is large and immobile, exhibits cation exchange properties and forms micelles. If some of the micelles can be doped or incorporated within the polymer matrix, then this would give a negatively charged surface that attracts cations and repels chloride anions. Furthermore, it has good solubility in aqueous solutions and it can be incorporated as a dopant during the electropolymerisation of pyrrole [23].

2. Experimental

The electrochemical experiments were carried out with a CH instruments (Model 760) potentiostat and a Solartron (Model 1287) potentiostat in conjunction with a Solartron frequency response analyser (Model 1255). The copper electrode was fabricated from a 4 mm diameter rod, which was encased in a Teflon holder. A copper wire was threaded into the base of the sample and used to connect to the potentiostat. A flat copper disc electrode was employed for SEM and EDX measurements. The electrodes were polished with successively lower sized diamond particles with a final polish using 1 μm diamond on a Buehler micro-cloth. The samples were then well rinsed with deionised water, sonicated and dried under a stream of air. A standard three electrode electrochemical cell was used with a saturated calomel electrode (SCE) and a high surface area platinum wire counter electrode. Current density, normalised to the geometric surface area of copper, is used in the polarisation and Tafel plots, while the currents presented for the formation of the polymer are not normalised, as the surface area of the polymer changes during growth.

The pyrrole monomer (98%) was obtained from Aldrich and was purified by distillation prior to use. It was then stored in the dark at −20 °C between experiments. The DBS solutions were prepared before each experiment and not stored as this gave poor reproducibility. Freshly prepared solutions gave good reproducibility, with nearly identical currents obtained during the formation of the PPy–DBS layers. All experiments were repeated at least three times and the average results are presented. The DBS doped polypyrrole films, PPy–DBS, were formed directly at copper or at an initial pre–layer of polypyrrole doped with tartrate to give a bilayer, PPy–Tar/PPy–DBS. The initial PPy–Tar layer was deposited from a neutral, pH of 7.0, solution containing 0.3 M pyrrole and 0.10 M sodium potassium tartrate at 0.75 V for 600 s. This polymer-modified electrode was then transferred to the DBS–containing solutions. Typically, the electropolymerisation solution consisted of a 0.3 M pyrrole and 0.05 M DBS solution and the polymer was formed at 0.75 V vs SCE for 600 s at the initial PPy–Tar film. The influence of the DBS concentration was studied by varying the DBS concentration from 9 mM to 0.1 M, while the impact of the electropolymerisation period and applied potential on the corrosion protection properties were investigated by altering the electropolymerisation period from 150 s to 1000 s and the applied potential from 0.70 V to 0.90 V vs SCE.

The surface morphology was studied using scanning electron microscopy (SEM) coupled with energy dispersive X–Ray analysis (EDX). The SEM measurements were performed on a Hitachi FE–scanning electron microscope, with an Oxford instruments Inca X–act 4.12 software package. The EDX analyses were carried out using an EDX Model 51–ADD0009 with the software package Micro Analysis Suite. Prior to the SEM measurements, a thin gold layer was deposited on the surface using an Emitech K550× gold sputter coater.

The corrosion protection properties were studied using polarisation curves, open–circuit potential measurements and Tafel plots. Polarisation curves were recorded in a near neutral (pH of 6.5) 0.1 M NaCl solution at 1 mV s^{-1} from an initial potential of −0.50 V vs SCE. Tafel plots were recorded at 0.17 mV s^{-1} in 0.1 M NaCl at pH 6.5. The electrodes were polarised from 175 mV below the corrosion potential. These data were fitted to the Tafel equation and used to estimate the corrosion potential, E_{corr}, and the corrosion current density, j_{corr}. Prior to recording these polarisation data the electrodes were immersed in the NaCl solution for 15 min to allow the potential to decay from the electropolymerisation potential. Impedance data were recorded as a function of time and at various applied potentials. A potential perturbation of 5 mV was used to ensure a pseudo–linear response, while the frequency was varied from 65 kHz to 6 mHz and a total of 10 points per decade were collected. The data were fitted to equivalent circuits, where the errors in the fitted element was less than 2.8%.

The conductivity measurements were carried out using a Jenway 4510 conductivity meter. The conductivity meter was calibrated using a 0.01 M KCl solution at 25 °C. The conductivity of DBS was measured in the presence and absence of 0.3 M pyrrole in deionised water maintained at 25 °C. The conductivity was measured after each addition of DBS. The solutions were agitated to facilitate mixing and the conductivity was measured after approximately a 2 min equilibration period. The CMC was estimated from the intersection of the two linear regions corresponding to the DBS anions, at lower concentrations, and the DBS micelles, which are formed at higher DBS concentrations.

3. Results and discussion

3.1. Formation of PPy–DBS and PPy–Tar/PPy–DBS

Polypyrrole doped with DBS was formed at a tartrate–doped polypyrrole film deposited at copper and it was also formed directly at copper. The tartrate system was selected as it gives a stable pre–layer of polymer that can be used to deposit the PPy–DBS film. The current–time plot recorded on application of 0.75 V vs SCE to the copper electrode in the pyrrole and tartrate–containing solution is shown in Fig. 1(a). The growth profile is typical for the electropolymerisation of pyrrole in a simple dopant solution. Some dissolution of copper occurs on application of the potential. However, once the polymer begins to nucleate at the surface, the dissolution of the copper substrate is inhibited and the current decays to about 1.0×10^{-5} A. No further increase in the current is observed, indicating that the deposited polymer prevents the dissolution of the copper substrate. The tartrate ion forms a complex with copper. At a pH of 7.0, the ion exists as $C_4H_4O_6^{2-}$ as the p*K*a value is 3.77. Ballesteros et al. [28] have carried out a thermodynamic analysis of the copper(II) –tartrate chloride system and

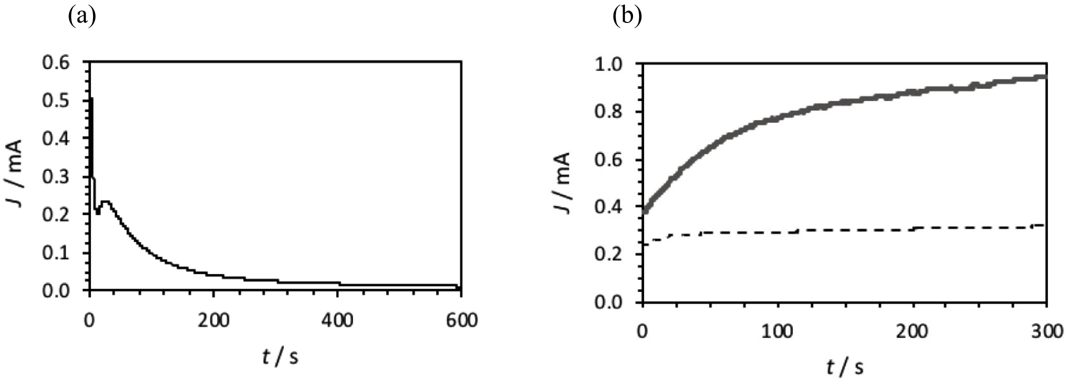

Fig. 1. Current–time plots recorded in (a) 0.1 M tartrate and 0.3 M pyrrole at 0.75 V vs SCE at Cu (b) 0.05 M DBS and 0.3 M pyrrole at PPy–Tar (formed for 600 s) at ▬ 0.90 V and ‒ ‒ ‒ 0.75 V vs SCE.

have shown that as the pH increases, there is a higher tendency for the formation of hydroxyl tartrate containing complex species, Equation (1). As the copper is dissolved initially and the Cu^{2+} ion concentration increases, this hydroxyl-tartrate complex is formed and this will limit the dissolution of copper.

$$Cu^{2+} + 2OH^{-} + 2C_4H_4O_6^{2-} \rightarrow Cu(C_4H_4O_6)_2(OH)_2^{4-} \qquad (1)$$

The formation of PPy–DBS at this PPy–Tar film at copper is shown in Fig. 1(b), where the polymer was formed at 0.75 V and 0.90 V vs SCE. The current reaches a near steady state at about 0.2 mA when polypyrrole is deposited at 0.75 V vs SCE and there is no further increase in the current. When the polymer is formed at the higher potential, the current increases indicating that the resistance of the PPy–Tar is sufficiently low to facilitate the electropolymerisation of the monomer and the formation of further layers of polypyrrole. These increasing currents are connected to the further deposition of polypyrrole giving a higher surface area and higher currents. EDX analyses were performed to determine if any copper dissolution occurred during this period. EDX spectra recorded for the bilayer polymer film deposited at 0.70 V and 0.90 V vs SCE are compared in Fig. 2. It is clearly evident, from the ratio of the sulfur to copper signal, that considerably more DBS is incorporated at 0.90 V vs SCE. This is consistent with the formation of a thicker polymer film at 0.90 V vs SCE. The PPy–Tartrate/PPy–DBS bilayer formed at 0.70 V vs SCE is sufficiently thin to observe X–Rays from the copper substrate. It is clear from the EDX spectrum in Fig. 2(b), that there is little evidence for dissolved copper ions within the polymer matrix. Although, the PPy–Tartrate film was polarised at 0.90 V vs SCE to deposit the PPy–DBS layer, there is no evidence to support the dissolution of copper and the generation of copper ions which are dispersed throughout the polymer matrix, which suggests that the increasing currents observed in Fig. 1(b) are indeed due to polymer formation.

In Fig. 3, current–time plots are shown for the electropolymerisation of pyrrole in 0.05 M DBS at an uncoated copper electrode at 0.70 V and 0.80 V vs SCE. The initial current, corresponding to the dissolution of copper, remains high for approximately 65 s for deposition at 0.80 V vs SCE. This active period depends on the applied potential, becoming longer at lower potentials where the rate of electropolymerisation is slower, reaching values of 180 s at 0.70 V vs SCE. Adherent polymer films were formed at the surface, however the formation of the polymer films depended on the pH of the solution, and these adherent films were only generated at a pH of approximately 6.0. More acidic pH values gave rise to more significant dissolution, while more alkaline values resulted in a much lower rate of electropolymerisation.

The active periods evident in Fig. 3 may be connected to a slow formation of a stable copper–DBS complex or to a relatively slow rate of electropolymerisation and this may be related to the micellar properties of DBS. In order to obtain information on this micelle–concentration relationship, the critical micelle concentration, CMC, of DBS in the absence and presence of pyrrole was determined using conductivity measurements. In Fig. 4, a typical conductivity measurement is shown, where the conductivity is plotted as a function of the BDS concentration in deionised water. Two linear regions are observed and the intersection point corresponds to the formation of micelles. The linear region at low DBS concentrations represents the DBS anions and no micelles are formed at these concentrations. As more DBS anions are added, the conductivity increases and this increase continues until the concentration reaches the CMC. Above the CMC micelles are formed and as these have a lower mobility, compared to the individual DBS anions, there is a change in the slope of the linear plot. Approximate

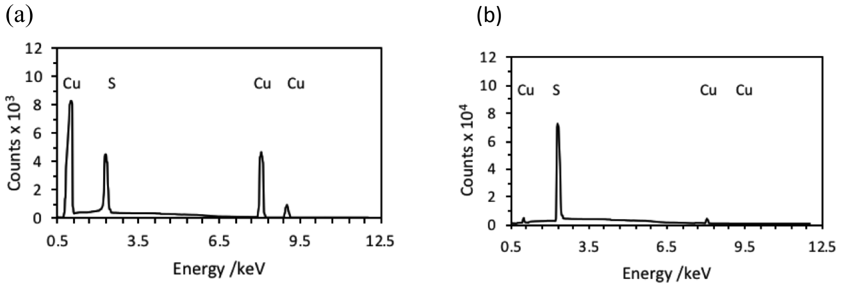

Fig. 2. EDX spectra of PPy–Tar/PPy–DBS with the PPy–DBS layer deposited from a 0.3 M pyrrole and 0.05 M DBS solution for 600 s and formed at (a) 0.70 V vs SCE and (b) at 0.90 V vs SCE.

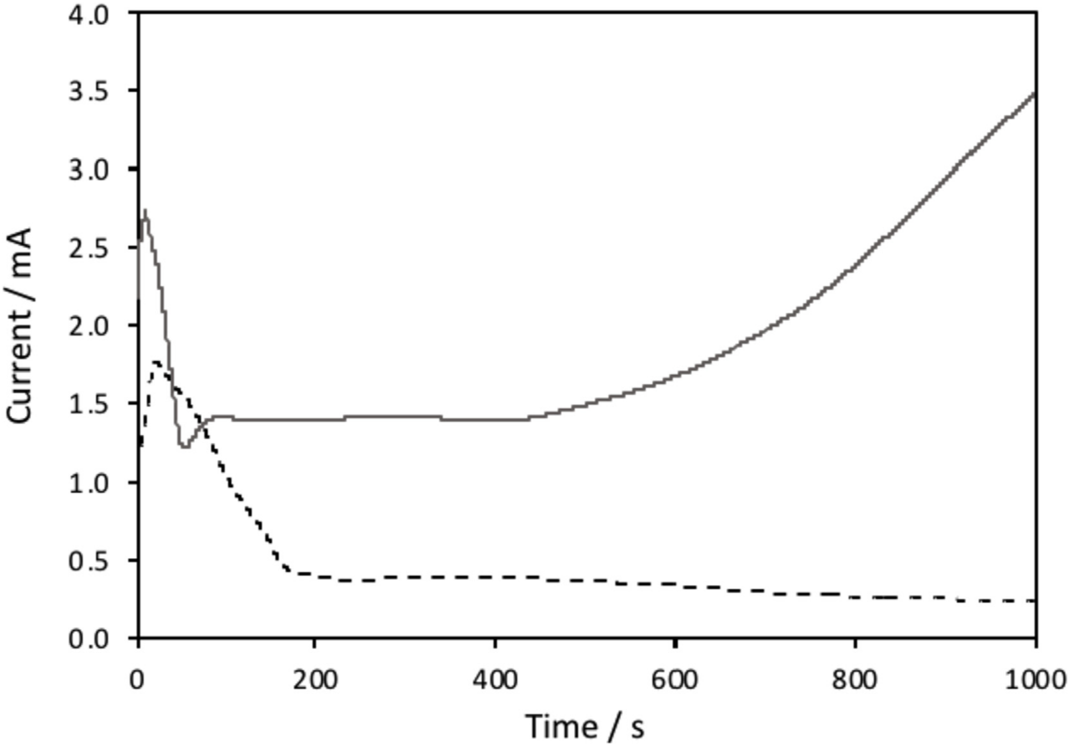

Fig. 3. Formation of PPy–DBS at copper in 0.05 M DBS and 0.3 M pyrrole at - - - 0.70 V and —— 0.80 V vs SCE.

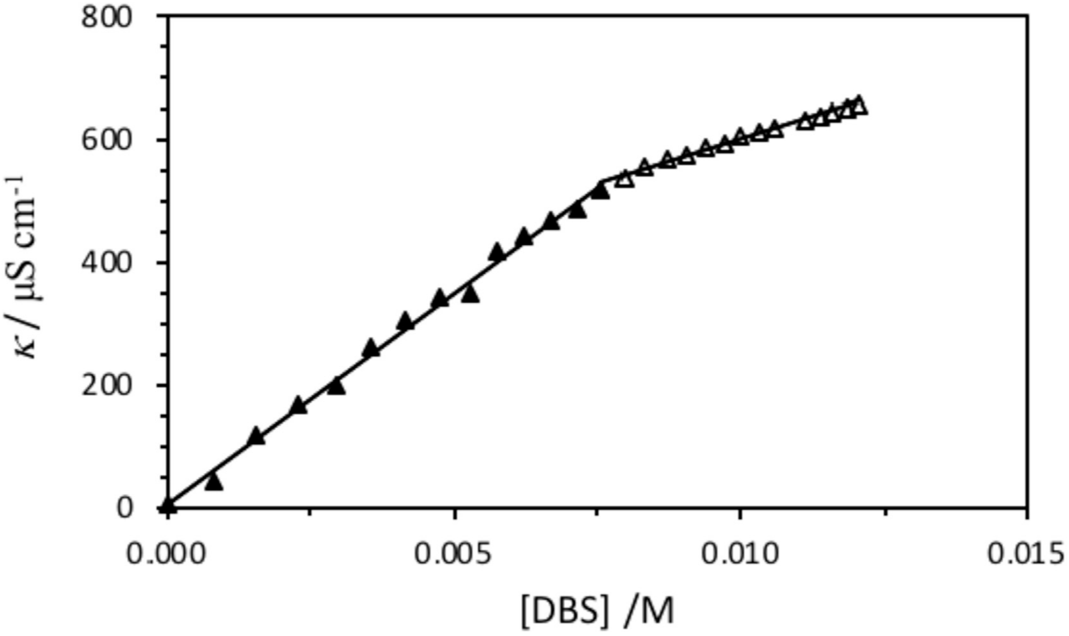

Fig. 4. Conductivity plotted as a function of the DBS concentration in deionised water.

CMC values of 7.8 mM and 9.8 mM were obtained in the absence and presence of pyrrole. This shows that the solutions formed at 0.05 M DBS contain a relatively high concentration of micelles. Although pyrrole is trapped within the micelles formed by the DBS [29], the concentration of pyrrole is well in excess of the DBS and there is sufficient pyrrole at the surface to enable electropolymerisation. It is more likely that the slow rate of electropolymerisation is connected with the adsorption of micelles. As the CMC is 9.8 mM, then a high concentration of micelles will exist in the 0.05 M DBS solution, giving rise to their adsorption at the copper surface. The adsorption of micelles has been described as admicelles or layers of micelles [29,30] and this interface may reduce the rate of electron transfer and limit the initial oxidation of the monomer. These effects have more influence at the uncoated copper where the two competing events of polymer nucleation and copper dissolution occur.

The influence of the DBS concentration on the morphology of the polymer bilayers is shown in Fig. 5. The PPy–DBS films were formed at the PPy–Tar layer at 0.75 V vs SCE for 600 s in solutions containing DBS at concentrations ranging from 1 mM to 0.10 M. It is clear that the concentration has a significant effect on the surface morphology. Uniform and homogeneous films were formed with DBS concentrations ranging from 10 mM to 0.10 M. The characteristic cauliflower morphology is seen at the higher DBS concentrations. The size and diameter of the cauliflower structures increase with increasing concentrations of DBS, with the highest diameters observed at 0.05 M and 0.10 M. As the concentration is lowered to 1.0 mM, oval-type structures, which appear to have voids, are formed. Although there are still a few cauliflower structures at this low concentration, the oval structures are in abundance. As the concentration of DBS is increased more dopants become available and more conducting solutions are formed and the electropolymerisation becomes more efficient.

It was also evident that less uniform coatings were formed at these lower concentrations. In Fig. 6, data are presented for the PPy–DBS bilayer deposited from 9 mM DBS, where the distribution of copper and oxygen are shown across the area highlighted. In this figure the darker areas represent lower levels of the element. The mapping profile for copper shows that more copper is detected at the base of the cauliflower structures, while the darker middle region, where the cauliflower structures are seen, give a lower count for copper. The oxygen signal shows an opposite trend, with lower levels of oxygen at the base of the cauliflower structure. There was little change in the sulfur count (not shown). These variations in the concentration of oxygen and copper indicate changes in the thickness of the bilayer film. The cross section presented in Fig. 6(d) highlights these variations in thickness. An average thickness of 1.8 ± 1.5 μm was obtained. Uniform films and mapping profiles were formed at the higher concentration of 0.05 M DBS. In this case, there was little evidence of copper and no variations in the oxygen and sulfur counts, indicating thicker and more uniform polymers. The bilayer thickness was estimated as 3.4 ± 0.2 μm.

3.2. *Corrosion protection properties*

The corrosion protection properties were studied in a near neutral (pH 6.5) 0.1 M NaCl solution using a combination of slow scan rate polarisation curves, open–circuit potential measurements and Tafel analyses, where the corrosion currents and corrosion potentials were estimated using the Tafel equation. Breakdown potentials were obtained from the polarisation curves and are useful in comparing the polymer coatings as they mark the potential where the oxide/coatings fail and dissolution of the substrate is seen.

A typical potentiodynamic polarisation curve, recorded at 1.0 mV s^{-1}, is shown in Fig. 7(a) where the protective properties of the PPy–Tar/PPy–DBS bilayer are compared with the uncoated copper and the PPy–DBS formed directly at copper. The outer PPy–DBS layer was formed at 0.75 V vs SCE for 600 s, while the film

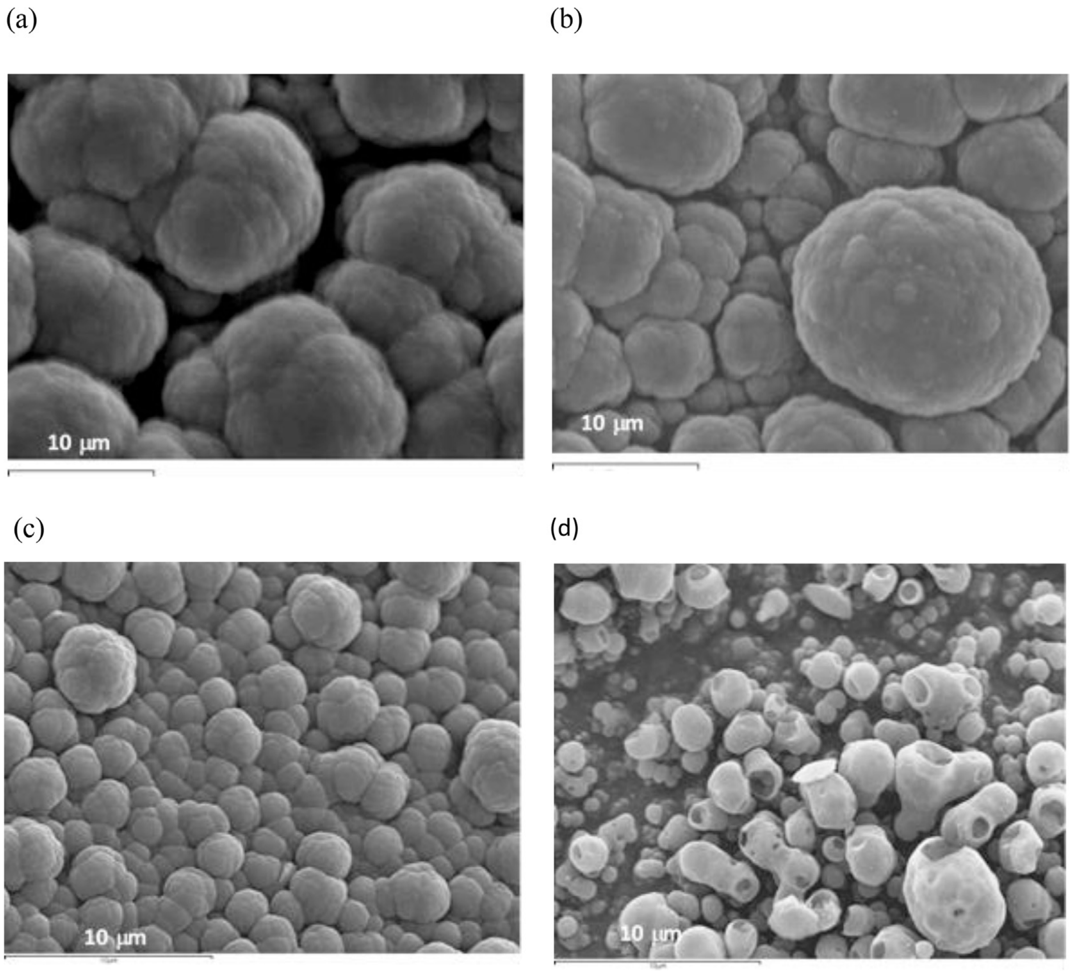

Fig. 5. SEM micrographs for PPy–Tar/PPy–DBS formed at 0.75 V vs SCE for 600 s in 0.3 M pyrrole and (a) 0.10 M DBS (b) 0.05 M DBS (c) 9.0 mM DBS and (d) 1.0 mM DBS.

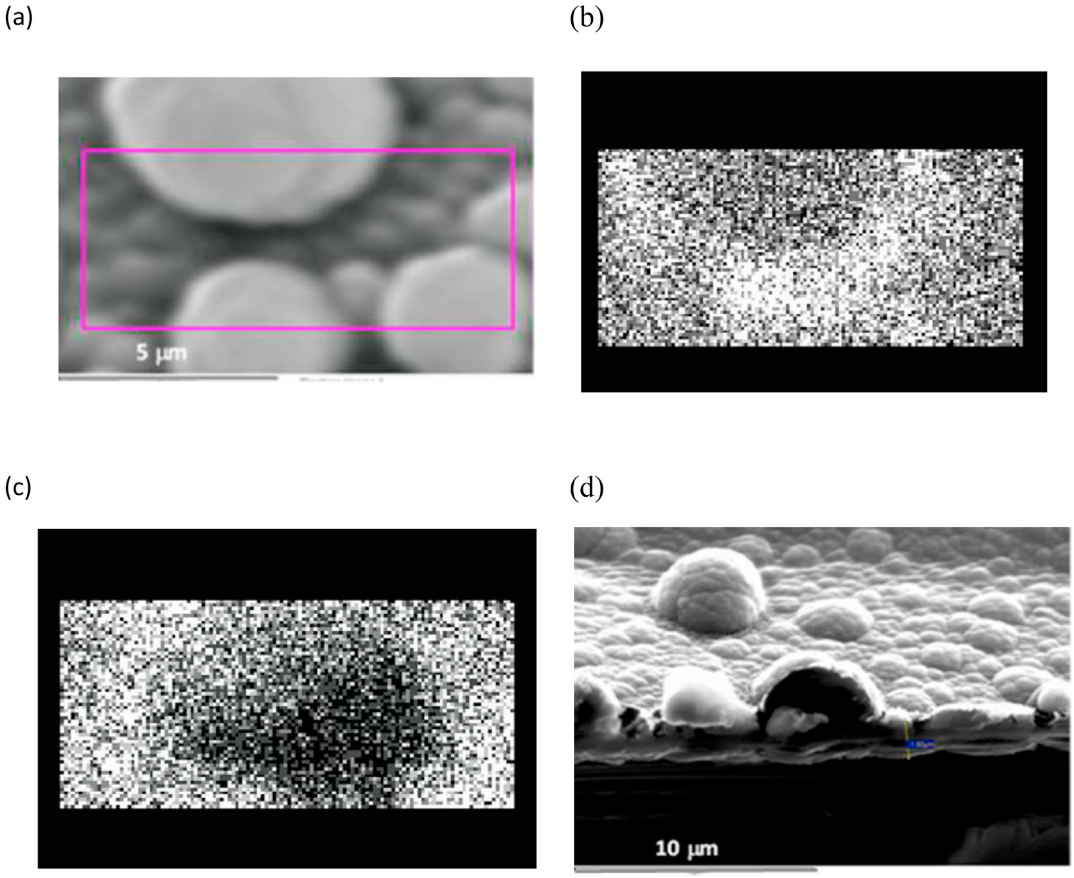

Fig. 6. SEM micrographs for PPy–Tar/PPy–DBS formed at 0.75 V vs SCE in 0.3 M pyrrole and 9.0 mM DBS for 600 s (a) area selected for mapping, (b) distribution of copper (c) distribution of oxygen and (d) cross section of polymer. The white coloured segments indicate the presence of the element.

formed directly at copper was deposited at 0.90 V vs SCE for 600 s and then at 0.75 V vs SCE for a further 600 s from a 0.3 M pyrrole and 0.05 M DBS solution. There is a significant difference between the voltammograms, with dissolution of the uncoated copper reaching a current of 1.0 mA cm^{-2} at approximately 0.10 V vs SCE. The protective properties of the polymer–coated copper are clearly evident with low currents and no indications of the dissolution of the copper substrate at 0.10 V vs SCE. The current begins to increase at about 0.90 V vs SCE for the PPy–Tar/PPy–DBS coating and this indicates breakdown of the polymer film and the dissolution of copper. The PPy–DBS film deposited directly at the copper electrode has a slightly lower breakdown potential of 0.86 V ± 0.30 vs SCE and the current begins to increase at about 0.20 V vs SCE and reaches current values of 0.1 mA cm^{-2} at 0.70 V vs SCE.

Although the difference in the breakdown potentials is relatively small between these two polymer systems, the PPy–Tar/PPy–DBS bilayer showed better protective properties. This may be related to the polypyrrole–metal interface. More dissolution of the copper was evident during the electropolymerisation of pyrrole in the DBS–containing solution at the pure copper surface, compared to the tartrate system, Figs. 1 and 3. Prissanaroon et al. [25] showed that an interfacial layer rich in sulfur was formed, indicating the presence of a DBS layer between the polymer and copper. Although initial dissolution is seen in the tartrate solution, the copper electrode is passivated more quickly limiting the thickness of this initial layer and this appears to give a slightly more protective surface. Indeed, the breakdown potential for the PPy–DBS films depended on the applied potential used to form the polymer, with values ranging from 0.86 V vs SCE at a formation potential of 0.90 V vs SCE to a much lower breakdown potential of 0.45 V vs SCE when the polymer was formed at 0.65 V vs SCE. As shown in Fig. 3, the active dissolution period remains considerably longer when the polymer is formed at a lower potential.

Polarisation curves, in the vicinity of the corrosion potential, were recorded at a scan rate of 0.17 mV s^{-1} in an attempt to reduce the charging current contribution from the polypyrrole and these data were used in the Tafel analysis. Representative plots for the bi–layer, where the outer PPy–DBS layer was formed in 0.3 M pyrrole and 0.05 M DBS at 0.75 V vs SCE for 600 s and 200 s, are shown in Fig. 7(b). It is evident from this plot that lower corrosion currents and higher corrosion potentials are recorded for the polymer formed for 600 s, indicating a more protective polymer film. The computed corrosion potential, E_{corr}, corrosion current density, j_{corr}, and Tafel slopes, b_a and b_c, are summarised in Table 1, where the more protective bilayer is compared with copper and the initial PPy–Tar layer. In this case, the initial PPy–Tar layer was formed for 1200 s to enable a more direct comparison with the bilayer. The Tafel slopes and corrosion current obtained for copper are in good agreement with the data obtained by Mansfeld et al. [31] for copper in chloride solutions. It is clear that lower j_{corr} values are computed for the PPy–Tar/PPy–DBS bilayer, coupled with more electropositive corrosion potentials. This is consistent with a reduction in the rate of the copper dissolution half reaction. It is also evident that the inner PPy–Tar layer has some protective properties, but it is the PPy–DBS outer layer that provides the protective properties.

The influence of the applied potential and the electropolymerisation period on the corrosion protection properties of the

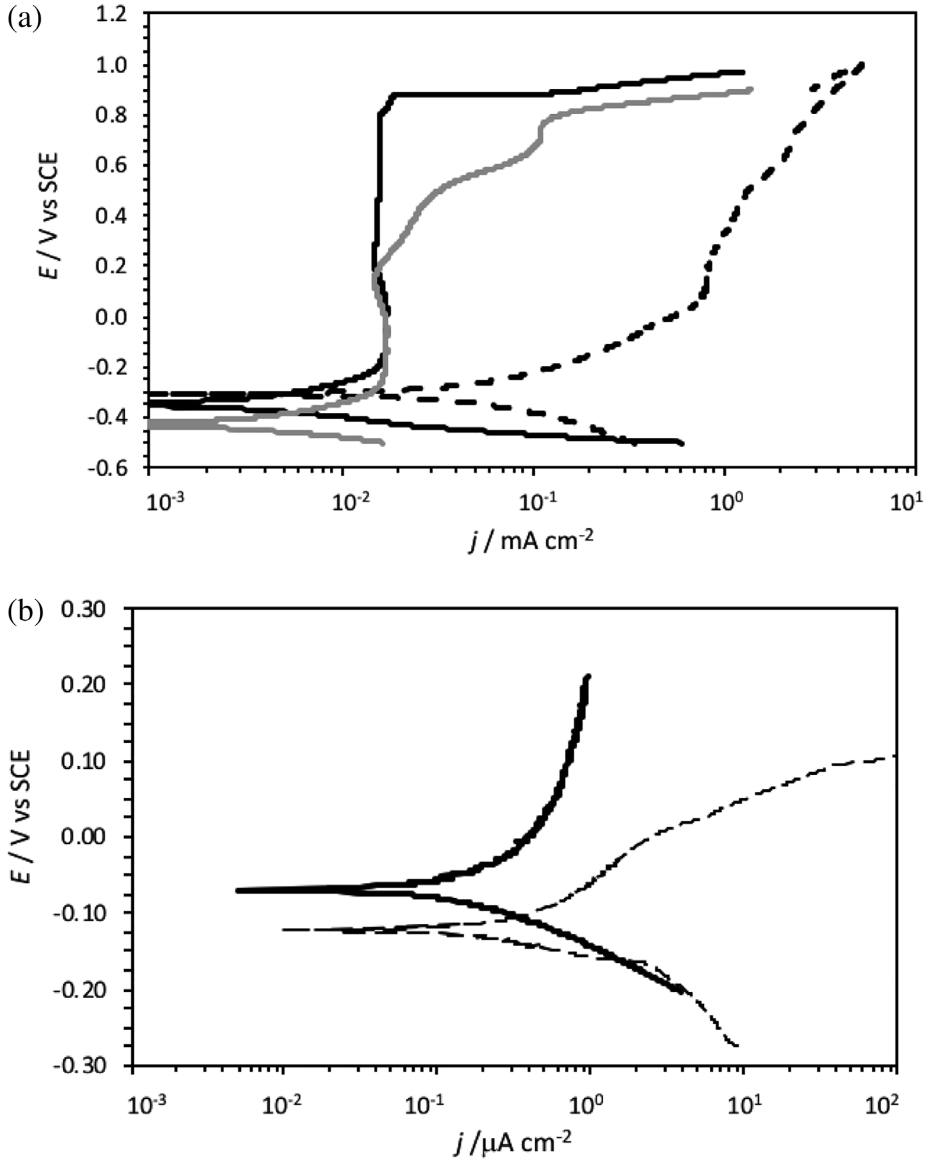

Fig. 7. (a) Potentiodynamic polarisation curves recorded at 1.0 mV s^{-1} in 0.1 M NaCl, pH 6.5 for – – – uncoated copper ▬ PPy–Tar/PPy–DBS (formed at 0.75 V vs SCE for 600 s at the PPy–Tar layer) and ▬ PPy–DBS coated copper where the PPy–DBS was deposited at 0.90 V vs SCE for 600 s and then at 0.75 V vs SCE for 600 s in 0.3 M pyrrole and 0.05 M DBS. (b) Tafel Plots recorded at 0.17 mV s^{-1} in 0.1 M NaCl for PPy–Tar/PPy–DBS with the PPy–DBS layer deposited from 0.3 M pyrrole and 0.05 M DBS at 0.75 V vs SCE for – – – 200 s and ▬ 600 s.

Table 1

Tafel slopes, E_{corr} and j_{corr} for uncoated and polymer–coated copper (n = 4). The PPy–Tar was formed in 0.3 M pyrrole and 0.1 M tartrate at 0.75 V vs SCE for 1200 s and the bilayer was formed at the PPy–Tar (600 s) in 0.3 M pyrrole and 0.05 M DBS at 0.75 V vs SCE for 600 s.

System	b_a/mV decade^{-1}	b_c/mV decade^{-1}	E_{corr}/V vs SCE	j_{corr}/μA cm^{-2}
Uncoated Cu	68	95	−0.245 ± 0.015	1.95 ± 0.03
PPy-Tar	91	48	−0.080 ± 0.030	1.70 ± 0.04
PPy-Tar/PPy-DBS	–	49	−0.065 ± 0.017	0.12 ± 0.03

polypyrrole bilayer were studied and these results are summarised in Table 2, where the breakdown and corrosion potentials are shown. The initial PPy–Tar film was deposited at 0.75 V vs SCE for 600 s, while the PPy–DBS outer layer was formed at potentials varying from 0.60 V to 0.90 V vs SCE and for time periods ranging from 100 to 1200 s. It is evident from Table 2 that protective bilayers, with high breakdown potentials and more electropositive corrosion potentials, can be formed by varying the potential and the electropolymerisation period. There is little difference in the protective properties of the bilayer, when the PPy–DBS layer is deposited at 0.75 V vs SCE for 400 s–1000 s. However, breakdown of the coating and dissolution of the copper substrate was observed for film deposition periods of 100 or 200 s. This shows that the thickness of the PPy–Tar/PPy–DBS, and in particular the thickness of the outer PPy–DBS layer, has an influence on the protective properties, with thin PPy–DBS layers providing less corrosion

Table 2
Influence of the electropolymerisation period and applied potential, E_{app}, on the breakdown, E_{b}, and corrosion potentials for PPy–Tar/PPy–DBS. The PPy–DBS layer was formed in 0.3 M pyrrole and 0.05 M DBS.

E_{app}/V vs SCE	t/s	E_{b}/V vs SCE	E_{corr}/V vs SCE
0.70	150	0.41 ± 0.08	−0.203
	300	0.81 ± 0.03	−0.110
	400	0.85 ± 0.02	−0.069
	600	0.91 ± 0.01	−0.075
	900	0.92 ± 0.01	−0.062
0.75	300	0.92 ± 0.02	−0.103
	600	0.93 ± 0.02	−0.065
0.80	300	0.91 ± 0.03	−0.081
	400	0.93 ± 0.02	−0.073
0.90	400	0.92 ± 0.02	−0.054
	1000	0.65 ± 0.10	−0.194

protection. For electropolymerisation at 0.90 V vs SCE, protective bilayer films were obtained at shorter times of 300 and 400 s, where the rate of electropolymerisation is higher. It is well known that electropolymerisation proceeds faster at higher applied potentials although the resistance of the films may increase due to over–oxidation of the polymer backbone [32]. However, at this relatively high potential, less protective polymer films were obtained at longer polarisation times. This suggests some over-oxidation of the polypyrrole film at these high applied potentials and longer polymerisation times to give a more open porous polymer film that facilitates the transport of chloride anions and dissolution of the copper substrate. Indeed, Lewis and co–workers [33] showed that over–oxidation of polypyrrole begins at 0.65 vs SCE, at pH 6.0, and becomes more significant at potentials higher than 0.80 V vs SCE.

The influence of the concentration of the DBS on the protective properties of the PPy–Tar/PPy–DBS bi–layer was studied by varying the concentration of the DBS in the electropolymerisation solution and these data are summarised in Table 3. It is clear that 0.05 M and 0.10 M solutions of DBS give the more protective polymer films. In all cases, the bilayer inhibits the dissolution of the copper substrate, but the breakdown and corrosion potentials depend on the concentration of DBS, with breakdown of the film observed at about 0.35 V vs SCE and lower corrosion potentials with 9 mM DBS, indicating poor corrosion protection properties. This is consistent with the data presented in Figs. 5 and 6 that show less efficient formation of the PPy–DBS bilayer at the lower DBS concentrations.

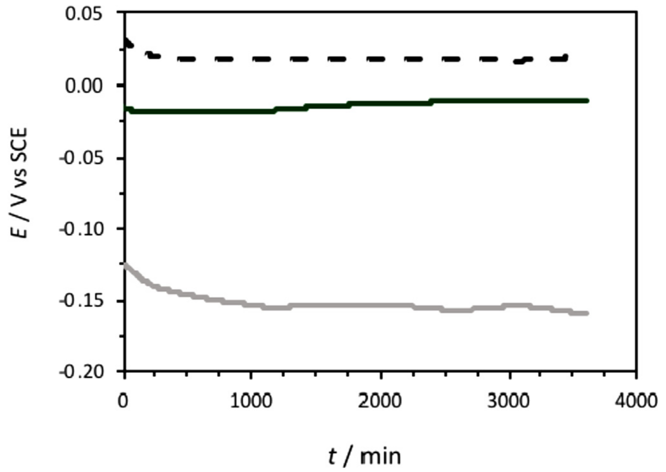

Fig. 8. Open–circuit potential recorded as a function of time in 0.1 M NaCl for ▬ copper, - - - PPy–Tar/PPy–DBS and ━ PPy–DBS. The PPy–DBS was formed at 0.75 V vs SCE for 600 s at the PPy–Tar layer (600 s) and at pure copper for 600 s at 0.90 V vs SCE followed by 600 s at 0.75 V vs SCE from a 0.3 M pyrrole and 0.05 M DBS solution.

Table 3
Influence of the DBS concentrations on the breakdown and corrosion potentials for PPy–Tar/PPy–DBS. The PPy–DBS layer was formed at 0.75 V vs SCE for 600 s in 0.3 M pyrrole.

Concentration/mM	E_{b}/V vs SCE	E_{corr}/V vs SCE
100	0.91 ± 0.02	−0.059
50	0.93 ± 0.02	−0.065
30	0.78 ± 0.03	−0.045
10	0.48 ± 0.05	−0.120
9	0.35 ± 0.07	−0.219

The open–circuit potential (OCP) of uncoated copper, PPy–DBS formed directly at copper and the PPy–DBS bilayer are shown as a function of time in Fig. 8. The polymers were placed in deionised water for a 20 min period to remove any unbound DBS and to allow the potential to decay from the electropolymerisation potential. The polymers were then transferred to a 0.1 M NaCl solution, without any prior polarisation. Therefore, the open–circuit potentials are more electropositive than the corrosion potentials, obtained from polarisation curves. The uncoated copper adopts potentials of about −0.15 V vs SCE, while higher values are recorded for the two polymer–coated electrodes. The open–circuit potential of the polymer–modified electrodes reach a near steady–state potential, that is always more noble that the potential recorded for the uncoated copper. There was little variation in this potential over a 30–day period and no evidence of any decay to the potential corresponding to the uncoated copper.

3.3. Impedance response of the PPy–Tar/PPy–DBS bilayer

Electrochemical impedance data were recorded for the PPy–Tar/PPy–DBS coated copper at potentials between −0.60 V and 0.60 V vs SCE. Steady–state conditions were achieved after approximately 200 min as shown in Fig. 9(a), where the impedance recorded at 0.01 Hz is shown as a function of the polarisation period at 0.40 V vs SCE. After this initial 200–min period, the impedance remains essentially constant indicating good stability over an extended polarisation period in a harsh chloride–containing solution. Impedance plots, where the impedance is shown as Bode plots, are presented in Fig. 9(b) and (c) for the PPy–Tar/PPy–DBS coated copper following a 200 min polarisation period in 0.1 M NaCl under open-circuit conditions ($E_{\mathrm{OCP}} = 20$ mV vs SCE) and at −0.50 V vs SCE. These data correspond to the oxidised or partially oxidised film that maintains the copper at more electropositive potentials, Fig. 8, and the reduced polymer that will exist in the event that the copper substrate undergoes dissolution. The OCP data were fitted to the equivalent circuit depicted in the figure, where Rs represents the solution resistance, R1 represents the charge–transfer resistance, and CPE1 and CPE2 are constant phase elements. Constant phase elements with a fractional exponent, n, give a measure of surface inhomogeneity, with n having values between 0.0 and 1.0 [34]. The higher exponent values, $n > 0.95$, point to a relatively high degree of surface homogeneity and correspond to a capacitor. Good agreement between the experimental and the fitted data was obtained as shown in the figure where the experimental data are compared to the fitted traces. The capacitance of the polymer at OCP was calculated as 30 mF cm^{-2} with an n value of 0.97 (CPE2), indicating a near ideal capacitor. These high capacitance values have been documented in previous reports and are normally associated with the conducting and charging properties of the polypyrrole film [35]. In contrast, the

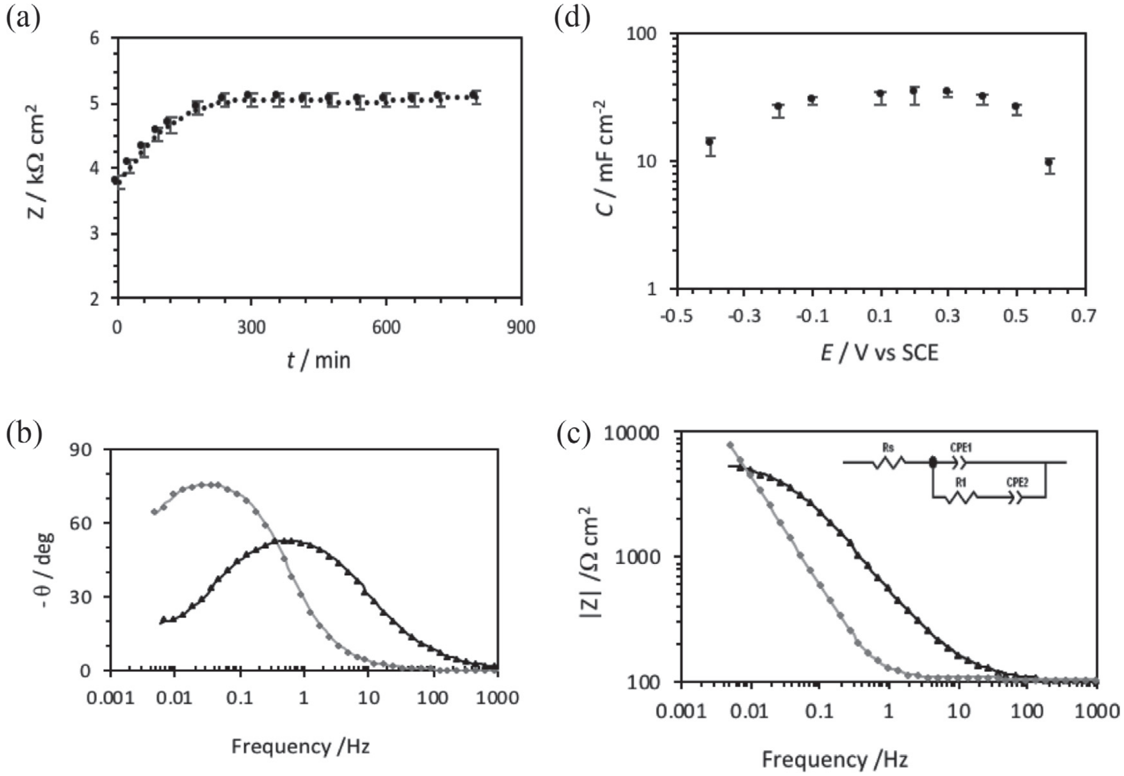

Fig. 9. Impedance data recorded for PPy–Tar/PPy–DBS (formed at 0.75 V vs SCE for 600 s at the PPy–Tar layer) in 0.1 M NaCl (a) impedance recorded at 0.40 V vs SCE at 0.01 Hz plotted as a function of time (n = 3) (b) and (c) Bode plots shown with experimental data as symbols recorded at Δ-Δ-Δ OCP and at ◆-◆-◆ −0.50 V vs SCE (d) capacitance plotted as a function of potential (n = 3).

capacitance of the uncoated copper electrode was calculated as 5.0 μF cm^{-2} when polarised at −0.20 V vs SCE, which is typical of double layer capacitance values recorded in chloride-containing electrolytes [36]. The charge-transfer resistance of the bilayer was estimated at 7 kΩ cm^2, which is somewhat higher than the value of 900 Ω cm^2 obtained for the bilayer formed at platinum (data not shown). On reduction of the polymer at −0.50 V vs SCE, the charge-transfer resistance increased to 25 kΩ cm^2, which is related to the formation of the reduced polymer, while the *n* value decreased to 0.85. The *n* value decreased further as the polymer was polarised to lower potentials, reaching approximately 0.5 at a potential of −0.60 V vs SCE. This indicates the development of a diffusional process, which is probably connected to the formation of PPy^o–DBS$^-$Na$^+$.

In Fig. 9(c), the capacitance of the PPy–Tar/PPy–DBS modified copper is shown as a function of the applied potential. The capacitance is essentially constant between 0.50 V and −0.20 V vs SCE, however, there is a reduction in the capacitance as the potential is increased to 0.60 V vs SCE. This decay in the capacitance is probably related to the over–oxidation of the polypyrrole matrix, resulting in the formation of a less conducting polymer substrate. There is also a reduction in the capacitance at potentials lower than −0.20 V vs SCE. This is consistent with the formation of the reduced PPy^o–DBS$^-$Na$^+$ film. It was not possible to estimate the capacitance at potentials lower than −0.40 V vs SCE, as the *n* value deviated too much from 1.0. These results show that the properties of the PPy–Tar/PPy–DBS film formed at copper are reasonably similar to polymers deposited at inert substrates, undergoing reduction at lower applied potentials and becoming over–oxidised as more electropositive potentials of 0.60 V vs SCE and higher are applied.

3.4. *Mode of corrosion protection*

It is evident from the data presented that copper is protected from dissolution in chloride-containing solutions by the PPy–Tar/PPy–DBS bilayer, at least for short immersion times. The mechanism by which polypyrrole protects metals and alloys from corrosion is not completely understood [37–39], with mechanisms varying from anodic protection, controlled inhibitor release, barrier protection to dislocation of the oxygen reduction reaction site to the conducting polymer. The anodic protection mechanism is described in several papers [37–39] and this is connected with the redox properties of the conducting polymer which maintain the underlying substrate in the passive domain. While this mechanism has been discussed for the protection of iron and iron-containing alloys it may also be relevant to the bilayer-coated copper.

Considering the Pourbaix diagram of copper [40], it is apparent that the electrode potential for the formation of Cu_2O, Equation (2), can be reached by the bilayer-coated copper, as shown in Fig. 8. Provided chloride anions are not present, then the copper substrate can be maintained as the Cu(I) oxide/hydroxide. However, as shown in Equation (3), the formation of CuCl is also thermodynamically viable and if this reaction occurs it may give rise to an acceleration of the corrosion reaction. Therefore, for the copper system, the removal of chloride anions is critical and the passive oxide is only maintained in the absence of chloride.

$$Cu_2O + 2H^+ + e^- \rightarrow 2\,Cu + H_2O \quad E = 0.471\text{–}0.0591\ \text{pH} \tag{2}$$

$$CuCl + e^- \rightarrow Cu + Cl^- \quad E = 0.157\ \text{V vs SHE} \tag{3}$$

The PPy–Tar/PPy–DBS bilayer has three phases, an inner tartrate-copper complex phase, the PPy-Tar layer, where the tartrate anion is largely a mobile anion and an outer PPy–DBS layer, where the DBS is immobile, giving rise to cation exchange. In addition, this outer layer may contain incorporated micelles. The CMC of DBS in the presence of pyrrole was estimated as 9.8 mM which is considerably lower than the 0.05 M DBS concentration employed in the formation of PPy-DBS. Indeed, Bay et al. [41] observed a large increase in the doping levels, obtained from mass changes, when alkyl benzenesulfonates, such as DBS, were used to form polypyrrole. This was explained by the incorporation of additional amounts of DBS, while Prissanaroon et al. [25] reported doping levels as high as 0.55 for DBS-doped polypyrrole films. As detailed earlier the capacitance of the bilayer is relatively high at 30 mF cm^{-2} and this may be connected to the incorporation of additional negative charge which is associated with the anionic micelles. This would also account for the observations made by Prissanaroon et al. and Bay et al. [25,41]. While the polymer is maintained in the oxidised state, this outer PPy–DBS layer will repel chloride anions with the immobile anionic DBS dopant and any incorporated anionic micelles. While equilibrium exchange at the polymer solution interface occurs between small mobile dopants and chloride anions in solution, the DBS is too large to facilitate exchange and it will remain incorporated as a dopant in the outer polymer layer. Under these conditions the chloride anion is repelled and the Cu(1) oxide/hydroxide substrate remains stable.

However, the events which accompany the reduction of the polymer are also important in the protection of the copper substrate as reduction of the polymer occurs at any defect site where dissolution of copper takes place. As the two polymer layers exhibit different exchange behaviours, reduction of the polymer bilayer involves both cation ingress and anion release as illustrated in Equation (4). These reduction events appear to begin at about −0.20 V vs SCE, as illustrated by the changes in the capacitance of the polymer, Fig. 9(d). A much larger intake of Na^{+} occurs in the vicinity of −0.60 V vs SCE where a diffusional process becomes evident, with the exponent of the CPE approaching 0.5.

$$\mathrm{PPy}^{2n+}\text{–}\mathrm{Tar}^{2n-}/\mathrm{PPy}^{m+}\text{–}\mathrm{DBS}^{m\text{-}} + m\mathrm{Na}^{+} + b\mathrm{H_2O} + ze^{-} \rightarrow \mathrm{PPy}^{o}/\mathrm{PPy}^{o}\text{–}\mathrm{DBS}^{m\text{-}}m\mathrm{Na}^{+}b\mathrm{H_2O} + n\mathrm{Tar}^{2-} \quad (4)$$

The release of tartrate from the inner layer has the potential to repassivate active sites. As shown in Equation (1), the tartrate anion forms a stable hydroxyl tartrate containing complex with Cu^{2+}. Therefore, it appears that the protective properties observed in this study are largely due to the chloride repelling properties of the outer layer, which helps to maintain the Cu_2O oxide phase, and the inhibitor release properties of the inner layer. This inner layer also serves to reduce the mobility of Na^{+} cations that are incorporated at the outer layer. While exclusive anion release may not be achieved with the tartrate anion, the concentration of Na^{+} incorporated within this layer will be relatively low as the dominant process is tartrate release. Rohwerder and Michalik [38] have shown that cation transport in anion–doped polypyrrole is fast, as the cations can hop between adjacent fixed negative charges. As the tartrate anions are released and the polymer backbone is reduced to the neutral polymer the transport of cations within this inner layer is reduced considerably. The ingress of Na^{+} and its associated solvated water molecules can lead to structural damage within the polypyrrole matrix [42]. The presence of an inner layer, that minimises the uptake and transport of Na^{+}, will possibly prevent these changes at the polymer–copper interface, reducing the risk of polymer delamination at the corroding site.

4. Conclusions

Protective polypyrrole coatings were formed on copper by electropolymerisation of pyrrole in the presence of DBS. The polymers were formed directly at copper from a 0.05 M DBS and 0.3 M pyrrole solution adjusted to a pH of 6.0. The polymers were also formed at an initial polypyrrole film generated from a tartrate solution to form a bilayer, PPy–Tar/PPy–DBS at the copper electrode. The bilayers were more protective and this was attributed to the copper–polypyrrole interface. In the presence of tartrate, the polypyrrole film formed readily without significant dissolution of copper, while considerably more copper was dissolved prior to the nucleation and growth of the polypyrrole layer in the presence of DBS. The concentration of DBS had an influence on the morphology and the protective properties of the polypyrrole films. More protective bilayer films, with a breakdown potential of 0.93 V vs SCE, were obtained using a 0.05 M DBS solution. The applied potential and the electropolymerisation period, which influence the thickness of the polymer films, were also found to affect the breakdown potentials and corrosion potentials. The corrosion protective properties were attributed to the immobile nature of DBS which is retained within the polymer on reduction due to its large size and the polymer film exhibits cation exchange properties. Furthermore, DBS forms micelles at concentrations higher than 9.8 mM and some of these micelles are likely to dope the polymer, or become incorporated within the polymer matrix, to give a negatively charged surface that repels anions.

Acknowledgements

The authors would like to acknowledge funding from the Research Frontiers Programme, Science Foundation Ireland.

References

[1] Y. Feng, K.S. Siow, W.K. Teo, K.L. Tan, A.K. Hsieh, Corrosion mechanisms and products of copper in aqueous solutions at various pH values, Corrosion 53 (1997) 389–398.
[2] D.W. Shoesmith, T.E. Rummery, D. Owen, W. Lee, Anodic oxidation of copper in alkaline solutions. I. Nucleation and growth of cupric hydroxide films, J. Electrochem. Soc. 123 (1976) 790–799.
[3] J.G.N. Thomas, A.K. Tiller, Formation and breakdown of surface films on copper in sodium hydrogen carbonate and sodium chloride solutions: effects of anion concentrations, Br. Corrosion J. 7 (1972) 256–262.
[4] G.K. Gomma, Effect of azole compounds on corrosion of copper in acid medium, Mater. Chem. Phys. 56 (1998) 27–34.
[5] M. Metikos-Hukovic, R. Babic, Z. Petrovic, D. Posavec, Copper protection by a self-assembled monolayer of alkanethiol, comparison with benzotriazole, J. Electrochem. Soc. 154 (2007) C138–C143.
[6] A.M. Fenelon, C.B. Breslin, The electrochemical synthesis of polypyrrole at a copper electrode: corrosion protection properties, Electrochim. Acta 47 (2002) 4467–4476.
[7] A.M. Fenelon, C.B. Breslin, The electropolymerisation of pyrrole at a CuNi electrode: corrosion protection properties, Corrosion Sci. 4 (2003) 2837–2850.
[8] M.I. Redondo, C.B. Breslin, Polypyrrole electrodeposited on copper from an aqueous phosphate solution: corrosion protection properties, Corrosion Sci. 49 (2007) 1765–1776.
[9] V. Annibaldi, A.D. Rooney, C.B. Breslin, Corrosion protection of copper using polypyrrole electrosynthesised from a salicylate solution, Corrosion Sci. 59 (2011) 179–185.
[10] M.M. Gvozdenovic, B.Z. Jugovic, J.S. Stevanovic, B. Grgur, T.L. Trisovic, Z.S. Jugovic, Electrochemical synthesis and corrosion behaviour of polyaniline–benzoate–coating on copper, Synth. Met. 161 (2011) 1313–1318.
[11] A.C. Cascalheira, S. Aeiyach, P.C. Lacaze, L.M. Abrantes, Electrochemical synthesis and redox behaviour of polypyrrole coatings on copper in salicylate aqueous solution, Electrochim. Acta 48 (2003) 2523–2529.
[12] Y. Lei, N. Sheng, A. Hyono, M. Ueda, T. Ohtsuka, Influence of pH on the synthesis and properties of polypyrrole on copper from phytic acid solution for corrosion protection, Prog. Org. Coatings 77 (2014) 774–784.
[13] Y. Lei, N. Sheng, A. Hyono, M. Ueda, T. Ohtsuka, Electrochemical synthesis of polypyrrole films on copper from phytic solution for corrosion protection, Corrosion Sci. 76 (2013) 302–309.
[14] Y. Lei, T. Ohtsuka, N. Sheng, Corrosion protection of copper by polypyrrole film studied by electrochemical impedance spectroscopy and the electrochemical quartz microbalance, Appl. Surf. Sci. 357 (2015) 1122–1132.
[15] M.I. Redondo, E. Sanchez de la Blanca, M.V. Garcia, M.J. Gonzalez–Tejera, Poly(Nmethylpyrrole) electrodeposited on copper: corrosion protection

properties, Prog. Org. Coatings 65 (2009) 386–391.

[16] I. Çakmakci, B. Duran, G. Bereket, Influence of electrochemically prepared poly (pyrrole–co–N-methyl pyrrole) and poly(pyrrole)/poly (N–methyl pyrrole) composites on corrosion behavior of copper in acidic medium, Prog. Org. Coatings 76 (2013) 70–77.

[17] B. Duran, G. Bereket, Cyclic voltammetric synthesis of poly (N–methyl pyrrole) on copper and effects of polymerisation parameters on corrosion performance, Ind. Eng. Chem. Res. 51 (2012) 5246–5255.

[18] V. Shinde, S.R. Sainkar, P.P. Patil, Corrosion protective poly(o–toluidine) coatings on copper, Corrosion Sci. 47 (2005) 1352–1369.

[19] P. Pawar, A.B. Gaikwad, P.P. Patil, Corrosion protection aspects of electrochemically synthesized poly(o-anisidine-co–o–toluidine) coatings on copper, Electrochim. Acta 52 (2007) 5958–5967.

[20] D. Patil, P.P. Patil, Electrodeposition of poly(o–toluidine) on brass from aqueous salicylate solution and its corrosion protection performance, J. Appl. Polym. Sci. 118 (2010) 2084–2091.

[21] A. Omrani, H. Rostami, R. Minaee, Electrochemical synthesis of polypyrrole/polyhedral oligomeric silsesquioxane nanocomposite on copper for corrosion protection, Prog. Org. Coatings 90 (2016) 331–338.

[22] H. Ozkazanc, S. Zor, Electrochemical synthesis of polypyrrole (PPy) and PPy-metal composites on copper electrode and investigation of their anticorrosive properties, Prog. Org. Coatings 76 (2013) 720–728.

[23] N. Aydemir, P.A. Kilmartin, J. Tracas–Sejdic, A. Keskula, A.L. Peikolainen, J. Parcell, M. Harjo, A. Aabloo, R. Kiefer, Electrolyte and solvent effects in PPy/DBS linear actuators, Sens. Actuators B Chem. 216 (2015) 24–32.

[24] N.T.L. Hien, B. Garcia, A. Pailleret, C. Deslouis, Role of doping ions in the corrosion protection of iron by polypyrrole films, Electrochim. Acta 50 (2005) 1747–1755.

[25] W. Prissanaroon, N. Brack, P.J. Pigram, J. Liesegang, Electropolymerisation of pyrrole on copper in aqueous media, Synth. Met. 142 (2004), 35–34.

[26] F. Wang, Z.Z. Jia, S.J. Luo, S.F. Fu, L. Wang, X.S. Shi, C.S. Wang, R.B. Guo, Effects of different anionic surfactants on methane hydrate formation, Chem. Eng. Sci. 137 (2015) 896–903.

[27] S. Chauhan, K. Sharma, Effect of temperature and additives on the critical micelle concentration and thermodynamics of micelle formation of sodium dodecyl benzene sulfonate and dodecyltrimethylammonium bromide in aqueous solution: a conductometric study, J. Chem. Thermodyn. 71 (2014) 205–211.

[28] J.C. Ballesteros, E. Chainet, P. Ozil, Y. Meas, G. Trejo, Electrodeposition of copper from non-cyanide alkaline solution containing tartrate, Int. J. Electrochem. Sci. 6 (2011) 2632–2651.

[29] K. Naoi, Y. Oura, M. Maeda, S. Nakamura, Electrochemistry of surfactant–doped polypyrrole film (I): formation of columnar structure by electropolymerisation, J. Electrochem. Soc. 142 (1995) 417–422.

[30] T. Pongprayoon, N. Yanumet, E.A. O' Rear, Admicellar polymerization of styrene on cotton, J. Colloid Interface Sci. 249 (2002) 227–234.

[31] F. Mansfeld, Tafel slopes and corrosion rates obtained in the pre–tafel region of polarisation curves, Corrosion Sci. 47 (2005) 3178–3186.

[32] D.A. Kaplin, S. Qutubuddin, Electrochemically synthesized polypyrrole films: effects of polymerisation potential and electrolyte type, Polymer 36 (1995) 1275–1286.

[33] W.T. Lewis, G.G. Wallace, Y.C. Kim, D.Y. Kim, Studies of the overoxidation of polypyrrole, Synth. Met. 84 (1997) 403–404.

[34] E. Barsoukov, J. Macdonald, in: E. Barsoukov, J. Macdonald (Eds.), Impedance Spectroscopy: Theory, Experiment, and Applications, second ed., John Wiley and Sons, 2005.

[35] X. Ren, P.G. Pickup, Impedance measurements of ionic conductivity as a probe of structure in electrochemically deposited polypyrrole films, J. Electroanal. Chem. 396 (1995) 359–364.

[36] A.V. Benedetti, P.T.A. Sumodjo, K. Nobe, P.L. Cabot, W.G. Proud, Electrochemical studies of copper, copper–aluminium and copper–aluminium–silver alloys: impedance results in 0.5 M NaCl, Electrochim. Acta 40 (1995) 2657–2668.

[37] P.P. Deshpande, N.G. Jadhav, V.J. Gelling, D. Sazou, Conducting polymers for corrosion protection: a review, J. Coating Technol. Res. 11 (2014) 473–494.

[38] M. Rohwerder, A. Michalik, Conducting polymers for corrosion protection: what makes the difference between failure and success? Electrochim. Acta 53 (2007) 1300–1313.

[39] G. Paliwoda-Porebska, M. Rohwerder, M. Stratmann, U. Rammelt, L.M. Duc, W. Plieth, Release mechanism of electrodeposited polypyrrole doped with corrosion inhibitor anions, J. Solid State Electrochem. 10 (2006) 630–736.

[40] M. Pourbaix, Applications of electrochemistry in corrosion science and in practice, Corrosion Sci. 14 (1974) 25–82.

[41] L. Bay, N. Mogensen, S. Skaarup, P. Summer-Larsen, M. Jorgensen, K. West, Polypyrrole doped with alkyl benzenesulfonates, Macromolecules 35 (2002) 9345–9351.

[42] E.M. Ryan, C.B. Breslin, Formation of polypyrrole with dexamethasone as a dopant: its cation and anion exchange properties, J. Electroanal. Chem. 824 (2018) 188–194.